Lagrange point stability for a rotating host mass binary

Martin D. Strong*
Department of Physics and Astronomy, Louisiana State University, Baton Rouge, Louisiana 70803, USA

Michael Crescimanno
Department of Physics and Astronomy, Youngstown State University, Youngstown, Ohio 44555, USA

(Received 2 January 2020; accepted 28 May 2020; published 16 July 2020)

In this new era of gravitational wave astrophysics, observations indicate the likely existence of black holes with significant spin. In order to better understand the potential imprint orbital dynamics have on the multimessenger data, we include rotation of the primary mass to leading order in the analysis of the stability boundary pertaining to the triangular equilibrium points, L_4 and L_5, in the relativistic, restricted, circular, three-body problem. For Lagrange point stability, these rotation effects are of the same order as the leading order relativistic corrections ignoring rotation, and they make both L_4 and L_5 more stable for retrograde orbital motion.

DOI: 10.1103/PhysRevD.102.024052

I. INTRODUCTION

The recent advent of gravitational wave astronomy and a maturing multimessenger methodology have contributed some urgency for a more thorough understanding of multicenter relativistic orbital systems. One important difference relativity introduces into the Newtonian class of problems is that the causal structure and therefore dynamics depend on the spin of objects, not just their masses. Incorporating the effects of a gravitating mass's angular momentum into spacetime structure and computing the orbital consequences on a test mass is well understood theoretically [1,2]. Furthermore, recent gravitational wave events [3] have also provided experimental signatures consistent with the coalescence and formation of rapidly spinning compact objects, which appear to be near the upper limits predicted by relativity. The planar relativistic two-body problem has also been extensively studied theoretically [4–7], and its numerical applications, including gravitational radiation, play key roles in interpreting experimental gravitational wave data.

Studying the classical restricted (planar, third mass is a test mass) three-body problem [8] is valuable for extending one's intuition, particularly for insight into the (leading order) general relativistic context [9–17]. Our goal here is to elucidate how angular spin momentum J of the "host" mass M influences the stability of the equilateral Lagrange points, L_4 and L_5, in the circular relativistic restricted three-body system. Understanding this case is of interest, as declared at the conclusion of the recent paper [16], "Coupled with the nondegenerate orbital frequencies of test particles in a Kerr background, the inclusion of spinning BHs would introduce many new degrees of freedom that may affect the stability of L_4 and L_5."

This article summarizes an approach and findings regarding this question. The main conclusion, limited to a binary system where the primary's (the larger mass's) spin axis is orthogonal to the orbital plane, is that L_4 and L_5's stability is degraded by prograde orbital motion but enhanced in the case of retrograde. Beyond being a new observation of potential relevance pertaining to accretion signals originating from compact binary systems, we suggest that the effect of rotation of the masses on the orbital stability of these admittedly idealized systems (planar, near circular orbits) fits into a larger narrative.

In Sec. II, we review relevant prior work regarding the relativistic restricted three-body problem and describe how to extend it to the case of a rotating primary. This leads to a pair of nonlinear differential equations which we integrate numerically and, specializing to the linear response theory about the equilibrium points, organize and summarize their stability criteria in Sec. III. Section IV concludes by providing a brief analytical narrative that places this stability result, and others, for the restricted two-body relativistic case in context.

II. ANALYTICAL DESCRIPTION

In order to investigate the stability of the Lagrange points in the relativistic, restricted, three-body problem, we begin with the approximate (to leading order, e.g., neglecting gravitational radiation) two-body relativistic system. The existing literature has several formulations of this system [4–7,9–13], although the vast majority do not include the effects of host mass rotation. We work to the leading order of small mass ratio, $m/M \ll 1$, by modifying the equations

*mdstrong.astrphys@gmail.com

of motion (EOM) of Huang and Wu [11] to include the angular momentum J of M. In this limit, and for small $a = J/(Mc)$, the inclusion of host mass rotation changes the binary's orbital period. Furthermore, for a test mass located at L_4 and L_5, we find additional a-dependent terms to be included in the EOM of [11]. These terms change the location and stability criteria for the Lagrange points. In preceding literature, the orbital equations are rendered in a rotating (about the center of momentum) Cartesian coordinate the frame with rate

$$\Omega_\pm = \omega_0 + \omega_1/c^2 \pm |a|\omega_0^2, \tag{1}$$

where, hereafter, the upper and lower signs correspond to prograde and retrograde orbital motion, respectively. We also define the dimensionless quantities $\mu_1 = \frac{M}{M+m}$ and $\mu_2 = \frac{m}{M+m}$ and scale G such that the Keplerian rate for the binary is $\omega_0^2 = 1/R^3$, while the leading relativistic correction with $a = 0$ is $\omega_1 = (\mu_1\mu_2 - 3)/(2R)$ (see [11]).

Our starting point is Eqs. (13)–(16) from Huang and Wu [11], which are consistent with the First post-Newtonian approximation (1PN) equations in [18,9]. To orient the reader, these equations do not include rotation (i.e., $a = 0$) of the host body, no effects from gravitational radiation or frictional forces, nor any other perturbations. Furthermore, the binary is assumed to occupy a circular orbit. In the rotating Cartesian center-of-momentum coordinates, the host mass and secondary are located at $(X_1, 0)$ and $(X_2, 0)$, respectively, with separation $R = |X_1 - X_2|$. For completeness, we reproduce here the equation set [Eqs. (12)–(16)] of [11] for an infinitesimal third test mass

$$\ddot{X} - 2\Omega\dot{Y} - \Omega^2 X = 2\omega_0^2\omega_1/c^2 X - A_{0,3}X + A_{1,3} + P/c^2, \tag{2}$$

$$\ddot{Y} + 2\Omega\dot{X} - \Omega^2 Y = -2\omega_0^2\omega_1/c^2 Y - A_{0,3}Y + Q/c^2, \tag{3}$$

where we have implemented the set of constants $A_{n,m} = \frac{\mu_1 X_1^n}{d_1^m} + \frac{\mu_2 X_2^n}{d_2^m}$ with $d_{1,2} = \sqrt{(X - X_{1,2})^2 + Y^2}$. The remaining post-Newtonian corrections in P and Q to this order [Eqs. (15) and (16)] from [11] are

$$\begin{aligned} P = {} & 6\omega_0 A_{0,1}\left(\dot{Y} + \frac{\omega_0}{2}X\right) + \frac{\mu_1\mu_2}{R}\left(\frac{X - X_1}{d_1^3} + \frac{X - X_2}{d_2^3}\right) + \omega_0\left(4\dot{Y} + \frac{7\omega_0}{2}X\right)(A_{1,3}X - A_{2,3}) - \frac{7\omega_0^2}{2}A_{1,1} \\ & + (4A_{0,1} - (U^2 + 2A\omega_0 + \mathcal{R}^2\omega_0^2) + 4\dot{X}^2 - 5\omega_0\dot{X}Y + \omega^2 Y^2)(A_{0,3}X - A_{1,3}) - 3\omega_0 A_{0,1}(2\dot{Y} + \omega_0 X) \\ & + A_{0,3}(4\dot{Y} + \omega_0 X)(\dot{X} - \omega_0 Y)Y - \frac{3\omega_0^2}{2}(A_{2,3}X - A_{3,3}) + \frac{3\omega_0^2}{2}Y^2(A_{2,5}X - A_{3,5}), \end{aligned} \tag{4}$$

$$\begin{aligned} Q = {} & -A_{1,3}\left(3\dot{X}\,\dot{Y} + 7\omega_0 X\left(\dot{X} - \frac{\omega_0}{2}Y\right)\right) + \omega_0 A_{2,3}\left(4\dot{X} - \frac{5\omega_0}{2}Y\right) + \frac{\mu_1\mu_2}{R}Y\left(\frac{1}{d_1^3} + \frac{1}{d_2^3}\right) \\ & - (\dot{Y} - \omega_0 X)(\omega_0 Y - \dot{X})(A_{0,3}X - A_{1,3}) + A_{2,5}\frac{3\omega_0^2}{2}Y^3 \\ & + A_{0,3}[Y(4A_{0,1} - (U^2 + 2\mathcal{A}\omega_0 + \mathcal{R}^2\omega_0^2) + (\dot{Y} + \omega_0 X)^2) + 3(\dot{Y} + \omega_0 X)(X\dot{X} + Y\dot{Y})] \end{aligned} \tag{5}$$

where, as per [11], $U^2 = \dot{X}^2 + \dot{Y}^2$, $\mathcal{A} = \dot{Y}X - \dot{X}Y$ and $\mathcal{R}^2 = X^2 + Y^2$.

Integrating the weak field equations for the metric outside of a finite spinning mass M, of angular momentum J, leads to the weak field limit of the exterior Kerr solution in the usual inertial frame spherical coordinates (t, r, θ, ϕ) [19],

$$g_{\mu\nu} = \begin{bmatrix} 1 - r_s/r & 0 & 0 & ar_s/r \\ 0 & -1/(1 - r_s/r) & 0 & 0 \\ 0 & 0 & -r^2 & 0 \\ ar_s/r & 0 & 0 & -r^2\sin^2\theta \end{bmatrix} \tag{6}$$

where $r_s = 2GM/c^2$ and $a = J/(Mc)$ as before. Next, we consider orbits of a much smaller mass ($m \ll M$) in this spacetime. By symmetry, a planar circular orbit has a constant 4-velocity $\frac{dx^\alpha}{ds} = u^\alpha = (u^0, 0, 0, u^3)$ that solves the equations of motion. The components can be recast into two constants, akin to the energy $\tilde{E}$ and the angular momentum $\tilde{L}$ as ascribed to the mass m by an asymptotic observer,

$$u^0 = \frac{r\tilde{E}}{r - r_s} - \frac{ar_s\tilde{L}}{r^2(r - r_s)}u^3 = \frac{ar_s\tilde{E}}{r^2(r - r_s)} + \frac{\tilde{L}}{r^2}. \tag{7}$$

Therefore, in the sign convention of Eq. (7), the expression for the angular velocity with respect to asymptotic time for a single center system is

$$\frac{d\phi'}{dt} = \dot{\phi}' = \frac{\tilde{L}/r^2 + ar_s\tilde{E}/(r^2(r - r_s))}{r\tilde{E}/(r - r_s) - a\tilde{L}r_s/(r^2(r - r_s))}, \tag{8}$$

where $\phi' = \phi + \Omega$ is the angular coordinate in the lab frame [the inertial frame of Eq. (7), as seen from the BH

"center"], and Ω is the rotating frame rate. The Cartesian coordinates in the rotating frame are thus given by $X = r\cos(\phi) + X_1$ and $Y = r\sin(\phi)$. For purpose of clarity, it may be beneficial for the reader to think of the "velocity" $\dot{\phi}$ as small, since for most of the orbits we expect $\dot{\phi}' \sim \Omega$. For this reason, in terms of the rotating frame angle $\phi' = \phi + \Omega t$,

$$\dot{\phi} = \frac{(X - X_1)\dot{Y} - Y\dot{X}}{r^2}, \tag{9}$$

where, again, X and Y are Cartesian coordinates as seen in the frame rotating about the center of momentum (CM) at angular frequency Ω. Note that $r^2 = (X - X_1)^2 + Y^2$ is the (parameter) distance to the black hole.

We now expand Eq. (8) out to leading order in a (dropping's for clarity),

$$\dot{\phi} = (L/E)\frac{r - r_s}{r^3} + a\left(\frac{r_s}{r^3} + (L/E)^2\frac{r_s(r - r_s)}{r^6}\right) - \Omega. \tag{10}$$

Since [11] has already developed the relativistic corrections to leading order without rotation, we only need to focus here on the new terms that arise when rotation is included. Thus, we develop the radial equation of motion to leading order in a,

$$\ddot{r} - r(\dot{\phi}')^2 = -\frac{r_s}{2r^2} + \frac{ar_s}{r^2}\dot{\phi}'. \tag{11}$$

As expected, rewriting Eqs. (11) and (10) in the X and Y coordinates leads to the classical limit of Eqs. (13) and (14) of Ref. [11], amended only by terms proportional to a. For first and second derivatives, we have

$$r\dot{r} = (X - X_1)\dot{X} + Y\dot{Y} \quad \dot{\phi}' - \Omega = \frac{(X - X_1)\dot{Y} - Y\dot{X}}{r^2}, \tag{12}$$

and also

$$r^3\ddot{r} = r^2((X - X_1)\ddot{X} + Y\ddot{Y}) + Y^2\dot{X}^2 + (X - X_1)^2\dot{Y}^2 - 2(X - X_1)Y\dot{X}\,\dot{Y} \tag{13}$$

$$\frac{\mathrm{d}}{\mathrm{d}t}(r^2(\dot{\phi}' - \Omega)) = (X - X_1)\ddot{Y} - Y\ddot{X}. \tag{14}$$

To further simplify this result, it is useful to define the function that arises in Eq. (10); specifically, let $f(r) \equiv \frac{r_s}{r^3} + \frac{(L/E)^2 r_s(r - r_s)}{r^6}$ and denote $f' = \frac{\mathrm{d}f}{\mathrm{d}r}$. With this nomenclature, the time derivative of Eq. (10) becomes

$$(X - X_1)\dddot{Y} - Y\dddot{X} + 2\Omega((X - X_1)\ddot{X} + Y\ddot{Y}) = (L/E)r_s\dot{r}/r^2 + a\dot{r}(2rf + r^2f') + \cdots, \tag{15}$$

where we are assuming that the secular evolution of the ratio (L/E) in the full (restricted three-body) problem leads to subdominant terms, since m/M is assumed small. Furthermore, by using Eq. (14), the radial equation Eq. (11), in these coordinates becomes

$$(X - X_1)\ddot{X} + Y\ddot{Y} - r^2\Omega^2 - 2\Omega((X - X_1)\dot{Y} - Y\dot{X}) = -\frac{r_s}{2r} + \frac{ar_s}{r}(\Omega + ((X - X_1)\dot{Y} - Y\dot{X})/r^2) + \cdots, \tag{16}$$

where, again, the "…" represents all the higher order relativistic terms independent of a. Next, by forming linear combinations of Eqs. (15) and (16), the equations of motion are combined into a form closer to that of Eqs. (13) and (14) of Ref. [11]. Additionally, transforming into the rotating frame centered about $(X, Y) = (0, 0)$, one has

$$\ddot{X} = 2\Omega\dot{Y} + \Omega^2 X - \frac{r_s(X - X_1)}{2r^3} - \frac{a}{r^2}\left(Y\dot{r}(2rf + r^2f') - \frac{(X - X_1)r_s}{r}(\Omega + ((X - X_1)\dot{Y} - Y\dot{X})/r^2)\right) + \cdots, \tag{17}$$

with the other linear combination being

$$\ddot{Y} = -2\Omega\dot{X} + \Omega^2 Y - \frac{r_s Y}{2r^3} + \frac{a}{r^2}\left((X - X_1)\dot{r}(2rf + r^2f') + \frac{Yr_s}{r}(\Omega + ((X - X_1)\dot{Y} - Y\dot{X})/r^2)\right) + \cdots. \tag{18}$$

Equations (17) and (18) now contain the leading "a"-dependent terms rather than those from the change in Ω due to the pair's motion [see Eq. (1) a dependence]. The "…" indicate the leading order relativistic terms that are already in P and Q of Eqs. (4) and (5), respectively.

Regarding the function f, as defined in the text above Eq. (15), we note

$$\dot{r}(2rf + r^2f') = ((X - X_1)\dot{X} + Y\dot{Y}) \times \left(-\frac{r_s}{r^3} - (L/E)^2\frac{r_s(3r - 4r_s)}{r^6}\right). \tag{19}$$

Thus, during the integration of Eqs. (17) and (18), in which the lhs of Eq. (19) appears, one must continually update the (in the full system) quasiconstant L/E using Eq. (10). Since the terms in Eqs. (17) and (18) involving f are already of order a, for Eq. (19) it suffices to use

$$(L/E) = \frac{r^3}{(r - r_s)}(\dot{\phi} + \Omega) = \frac{r^3}{(r - r_s)}\left(\frac{X\dot{Y} - Y\dot{X}}{r^2} + \Omega\right), \tag{20}$$

which we square and include in Eq. (19) before finally using its lhs in Eqs. (17) and (18).

In addition to integrating the equations of motion in time, it is straightforward to numerically determine the linear stability of the system about the equilibrium positions in the rotating frame. To motivate this approach, we start with the familiar classical problem: a particle subject to a potential $\tilde{V}(\vec{x})$, for which we are looking for solutions that are static in some rotating frame, i.e., stable circular orbits. The generic two-dimensional Lagrangian in inertial coordinates, $\tilde{x}$, $\tilde{y}$, is given by $\mathcal{L} = \frac{1}{2}(\dot{\tilde{x}}^2 + \dot{\tilde{y}}^2) - \tilde{V}(\tilde{x}, \tilde{y})$, which in the rotating frame becomes $\mathcal{L} = \frac{1}{2}(\dot{x}^2 + \dot{y}^2) + \Omega(\dot{x}y - \dot{y}x) - \tilde{V}(x, y) + \frac{\Omega^2}{2}(x^2 + y^2)$. Thus, in terms of the new potential $V = \tilde{V} - \frac{\Omega^2}{2}r^2$, the EOM becomes

$$\ddot{\vec{x}} - 2\vec{\Omega} \times \dot{\vec{x}} + \nabla V = 0. \tag{21}$$

The full problem of concern here has the additional complexity that the relativistic terms in the potential $V(\vec{x}, \dot{\vec{x}})$ are velocity dependent. For studying the stability of Lagrange points in the rotating frame, it suffices to expand the EOM about the points $(\vec{x}^*)$ for which $\nabla V|_{x^*}(\vec{x}, 0) = 0$. The velocities with respect to the rotating frame are zero at $\vec{x}^*$ to this order. Expanding to leading order as a linear system, we have

$$\ddot{\vec{x}} + \mathcal{S}\dot{\vec{x}} + \mathcal{H}\vec{x} = 0, \tag{22}$$

where $\mathcal{H}_{ij} = \partial_i \partial_j V$ is the Hessian of the potential in the rotating frame, evaluated at the point $\vec{x}^*$ and $\mathcal{S}_{ij} = 2\Omega\epsilon_{ij} + \frac{\partial \partial_j V}{\partial \dot{x}_i}$.

Taking the ansatz $\vec{x} = \vec{A}e^{-\gamma t}$ for some nonzero constant vector $\vec{A}$ into Eq. (22) then leads to a quartic equation for γ,

$$\begin{aligned}\gamma^4 - (\mathcal{S}_{xx} + \mathcal{S}_{yy})\gamma^3 + (\mathcal{S}_{xx}\mathcal{S}_{yy} - \mathcal{S}_{xy}\mathcal{S}_{yx} + \mathcal{H}_{xx} + \mathcal{H}_{yy})\gamma^2 \\ - (\mathcal{H}_{xx}\mathcal{S}_{yy} + \mathcal{H}_{yy}\mathcal{S}_{xx} - \mathcal{H}_{xy}\mathcal{S}_{yx} - \mathcal{H}_{yx}\mathcal{S}_{xy})\gamma \\ + \mathcal{H}_{xx}\mathcal{H}_{yy} - \mathcal{H}_{xy}\mathcal{H}_{yx} = 0.\end{aligned} \tag{23}$$

Lastly, to find the stability boundary, one needs to only plot the (appropriate) roots of the discriminant Eq. (23). Next, we describe the numerical evaluation of the full EOM in Eqs. (17) and (18) used to create the zero locus of the discriminant of Eq. (23) and also used to compute the orbits in this case.

III. NUMERICAL SOLUTION

In general, the classical triangular equilibrium point locations shift due to the relativistic correction terms. Therefore, by rewriting Eqs. (17) and (18) into a system of four, first order, nonlinear differential equations, the resulting vector field's zeroes were determined using GNU Scientific Library's (GSL's) multidimensional root-finding routine. The particular routine implemented a modified version of the Powell hybrid algorithm, but replaced calls to the Jacobian with finite difference approximations. As expected, L_4 and L_5 shift together, maintaining mirror symmetry across the line connecting the principal masses. Furthermore, in the relativistic regime, the equilibrium points move nearly parallel to the principal axis toward the secondary mass. As prograde rotation increased, both $L4$ and $L5$ moved toward one another in the direction of the principal axis; however, retrograde orbital motion shifted the location of the points outwards (Fig. 1).

The second portion of the code solved the orbital equations [Eqs. (17) and (18)] for the motion of the test mass (Fig. 2). The host and secondary mass separation remained constant at one unit, while the total mass of the system was also fixed at one in gravitational units ($G_N = 1$). Starting at locations near the equilibrium points, a test particle's trajectory was evolved using an explicit Runge-Kutta Prince-Dormand (8, 9) integrator for 100,000 orbits. The errors produced in each step were held within an absolute error bound of 1e-15.

The third part of the code numerically computes the second derivatives of the orbital differential equation's vector field, in both position and velocity, the $\mathcal{S}_{ij}$ and $\mathcal{H}_{ij}$ of Eq. (22), at the Lagrange points L_4 and L_5 found by the first part of the code. These numerical derivatives are taken in a symmetric way to control numerical systematics.

As a first check, both the orbital simulation, as described above, and the linear stability analysis [numerical evaluation of the discriminant of Eq. (23)] reproduce the stability boundary for L_4 and L_5, namely, $\mu > \mu^*_{\text{classical}} = \frac{1}{2} - \frac{\sqrt{69}}{18} \sim 0.038521$ in the classical limit $1/c^2 \to 0$, the large distance limit of the full relativistic problem. A second check is

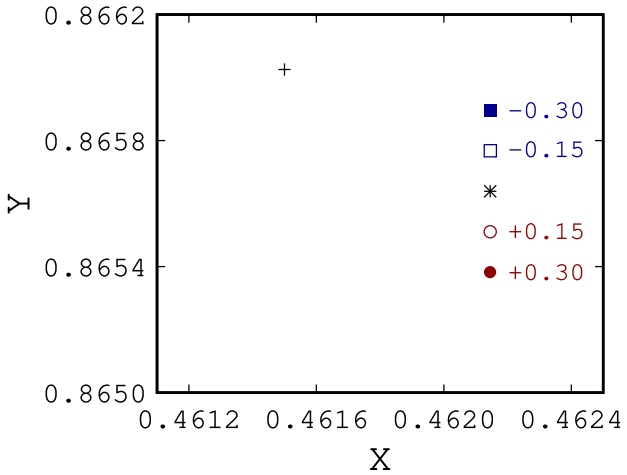

FIG. 1. The equilibrium points shift due to the relativistic correction terms. For $\mu = 0.0385$ the cross indicates the classical $(1/c^2 = 0)$ location of L4. The "Asterisk" is the Lagrange point for $c = 30$ but with $a = 0$. The other points are with this same c value but at the $a/a_{\max}$ values indicated.

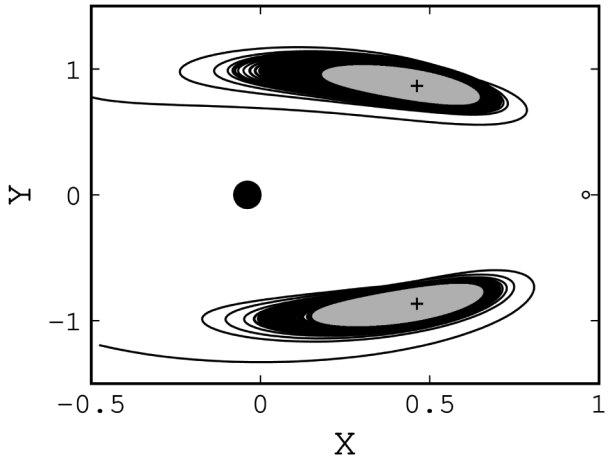

FIG. 2. Typical results of numerically integrating the EOM with $a = 0$. The center of mass of the system is located at the origin. The host mass is located at $(-\mu_2,0)$ and is much heavier than the secondary mass at $(\mu_1,0)$. The dark traces are representative of unstable orbits ($\mu > \mu^*_{\text{classical}}$) starting near $L4$ and $L5$. The light trace is similar, except for stable orbits ($\mu < \mu^*_{\text{classical}}$).

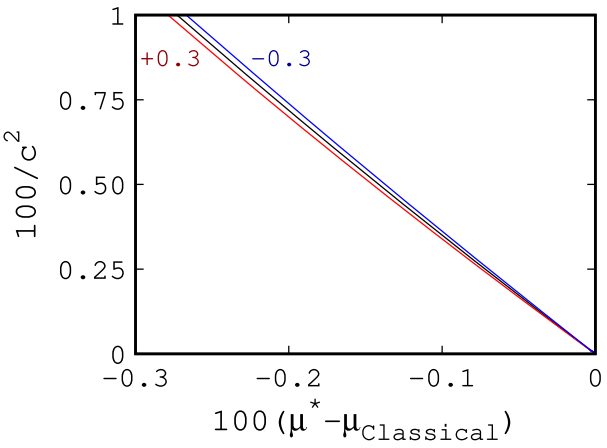

FIG. 3. Computed critical μ boundary versus $1/c^2 = r_s/(2r)$ for different J/M values for the host black hole. Each line corresponds to a particular critical binary; points above the lines are binaries that do not support stable $L4$, $L5$ orbits, whereas those corresponding to points below the line do have stable $L4, L5$ orbits. The x-axis is the classical (Newtonian) limit. The $J/M = 0$ computed curve (middle) is a line with slope $-17\sqrt{69}/486 = -0.29056$ as indicated in the literature [[18], Eq. (11)]. The surrounding lines, at the $a/a_{\max}$ values indicated, show that retrograde (negative) J/M binaries have stable $L4$ and $L5$ at larger mass ratios.

provided by comparing the $a = 0$ limit at nonzero $1/c^2$ from our code to the known analytical solution (Ref. [18]). That comparison indicates not only that the stability boundary at $a = 0$ should be a line but that the slope of the line should be $-17\sqrt{69}/486 \sim -0.29056$, which in the numerical method described here is reproduced to the leading six decimal places.

Using the method we have developed to study stability near the classical limit, but at finite $a = J/(Mc)$, we summarize the entire leading order relativistic stability boundary as (Fig. 3)

$$\mu^*(a,c) = \mu^*_{\text{classical}} - \frac{17\sqrt{69}}{972}\frac{r_s}{r} - 0.0355\frac{a}{r} + \cdots. \tag{24}$$

Note that although we have derived this in the small a limit, since $a < r_s/2$, we expect the rotation contribution to the stability boundary to always be smaller in magnitude than the leading relativistic term.

IV. DISCUSSION

The slip of the positions of L_4 and L_5 with respect to the nominal classical locations has a consistent trend that correlates with stability [20]. The energy level sets in the rotating frame are tear-drop shaped around each Lagrange point, with the steepest part of that potential at the section nearest the smaller of the two principal masses. Orbits near the Lagrange points in the stable regime explore the tear-drop shaped region, and as one increases the mass ratio to the stability boundary, the gradient of the potential in the part of the tear-shaped region nearest the secondary increases. The association of instability with the orbits navigating a region with larger gradients holds in both the post-Newtonian limit [11,13,18] and in the various dissipative variants of the classical problem [16,17,21]. In the post-Newtonian limit (with no rotation of the host mass), the shift of the Lagrange points towards the secondary is, in fact, a type of relativistic kinematical focusing.

Including the effects of rotation of the "host" mass M into the problem, we find, due to frame dragging, that a prograde orbit tends to shift L_4 and L_5 towards the axis between the bodies. Again, this increases the gradients of the potential near L_4 and L_5, thus making the system less stable. In a retrograde binary the opposite happens, leading to a greater stability near L_4, L_5.

The result that the Lagrange points are less stable in a prograde system than in a retrograde system appear counterintuitive with respect to the single-body case. Recall that for an isolated test mass revolving around a spinning black hole, for a given fixed parameter distance r, the prograde orbits have both higher frequency and smaller innermost stable circular orbits (ISCO) [22,23] than retrograde orbits. Recall further, the ISCO is the boundary between stable and unstable circular orbits for the relativistic case. Quite separately, in a generic parametric oscillator it is not unusual for (in the linearized picture) roots of the characteristic equation to merge with one another at or near zero frequency before the system becomes unstable (i.e., admit solutions of decaying amplitude). Both ISCO size and this eigenvalue flow thus indicate that the prograde system should be more stable than the retrograde one.

We can relieve the tension between this qualitative picture of stability and that of our findings for L_4 and L_5 for a rotating host in a binary pair by comparing the system's bound state energy in the $M \gg m$ limit. Note that the energy of the orbital system depends on the rotation parameter a. A brief calculation indicates that the asymptotically accorded total system energy for a circular orbit binary in the limit that the black hole mass M is much larger than the secondary (mass m) and in the limit of small a, is

$$E = M + \frac{m(1 - 2M/R - 2Ma\omega/R)}{\sqrt{1 - 3M/R - 6aM\omega/R}}, \tag{25}$$

where ω is the revolution rate, which in this $M \gg m$ limit in asymptotically inertial coordinates ($R \to \infty$) is

$$\omega = \omega_0 \pm |a|\omega_0^2, \tag{26}$$

where $\omega_0^2 = G(M + m)/R^3$ and the $\pm$ is for prograde or retrograde orbital motion, respectively. Combining Eqs. (25) and (26), we learn that the total energy of the retrograde system is always smaller than that of the prograde system in this limit (large R), all other factors being the same. We conjecture that this difference persists to all R. If so, the ISCO ordering (whereby the test mass is captured by the black hole) and the finding here (whereby the test mass at L_4 or L_5 is generically thrown out of the system) are consistent since this indicates that the retrograde system is more strongly bound than the equivalent prograde one.

Rather than always reducing the critical mass ratio for stability (as cited in earlier literature in the case of no rotation), relativistic effects due to the rotation of the host mass can actually increase the critical mass ratio (Fig. 3). If prograde orbital rotation is most likely astrophysical, then the foregoing suggests that the critical ratio for Lagrange point stability happens for even smaller mass ratios than allowed classically. As known from earlier work, for a light secondary paired with a rapidly spinning black hole host, motions of masses at L_4 and L_5 stable at large distances will become unstable as the binary shrinks and lead to ejection from the system for any rotation of the host mass.

ACKNOWLEDGMENTS

We wish to thank J. Schnittman for sharing his insights into the dynamics of the nonrotating case in leading nonrelativistic order and C. Johnson for discussion on the qualitative link between the findings and spacetime entropy change.

[1] J. Lense and H. Thirring, Über den einfluss der eigenrotation der zentralkrper auf die bewegung der planeten und monde nach der einsteinschen gravitationstheorie, Phys. Z. **19**, 156 (1918).
[2] R. P. Kerr, Gravitational Field of a Spinning Mass as an Example of Algebraically Special Metrics, Phys. Rev. Lett. **11**, 237 (1963).
[3] B. Zackay, T. Venumadhav, L. Dai, J. Roulet, and M. Zaldarriaga, Highly spinning and aligned binary black hole merger in the advanced ligo first observing run, Phys. Rev. D **100**, 023007 (2019).
[4] H. P. Robertson, Note on the preceeding paper: The two-body problem in general relativity, Ann. Math. **39**, 101 (1938).
[5] G. Contopolous, in *memorium D. Eginitis* (1976), p. 159.
[6] S. Chandrasekhar and G. Contopolous, On a post-Galilean transformation appropriate to the post-Newtonian theory of Einstein, Infeld and Hoffmann, Proc. R. Soc. A **298**, 123 (1967).
[7] T. Damour and A. Buonanno, Effective one-body approach to general relativistic two-body dynamics, Phys. Rev. D **59**, 084006 (1999).
[8] J. L. Lagrange, Essai sur le probleme des trois corps, Oeuvres de Lagrange **6**, 229 (1772).
[9] T. I. Maindl and R. Dvorak, On the dynamics of the relativistic restricted 3-body problem, Astron. Astrophys. **290**, 335 (1994).
[10] E. Krefetz, Restricted three body problem in the post-Newtonian approximation, Astrophys. J. **72**, 471 (1967).
[11] G. Huang and X. Wu, Dynamics of the post-Newtonian circular restricted three-body problem with compact objects, Phys. Rev. D **89**, 124034 (2014).
[12] B. Sicardy, Stability of the triangular Lagrange points beyond Gascheaus value, Celestial Mech. Dyn. Astron. **107**, 145 (2010).
[13] O. Ragos, E. A. Perdios, V. S. Kalantonis, and M. N. Vrahatis, On the equilibrium points of the relativisitic restricted three-body problem, Nonlinear Anal. Theory Methods Appl. **47**, 3413 (2001).
[14] K. Yamada and H. Asada, Triangular solution to the general relativistic three-body problem for general masses, Phys. Rev. D **86**, 124029 (2012).
[15] K. Yamada, T. Ichita and H. Asada, Post-Newtonian effects on Lagranges equilateral triangular solution for the three-body problem, Phys. Rev. D **83**, 084026 (2011).
[16] J. D. Schnittman, The Lagrange equilibrium points L_4 and L_5 in a black hole binary system, Astrophys. J. **724**, 39 (2010).
[17] J. Singh and N. Bello, On the stability of $L_{4,5}$ in the relativistic R_3BP with radiating Secondary, J. Astrophys. Astron. **35**, 685 (2014).
[18] C. N. Douskos and E. A. Perdios, On the stability of equilibrium points in the relativistic restricted three-body problem, Celestial Mech. Dyn. Astron. **82**, 317 (2002).

[19] L. D. Landau and E. M. Lifshitz, *The Classical Theory of Fields* (Pergamon Press, New York, 1987).
[20] We are indebted to J. Schnittman for this observation and explanation.
[21] C. D. Murray, Dynamical effects of drag in the circular restricted three-body problem, Icarus **112**, 465 (1994).
[22] See https://en.wikipedia.org/wiki/Innermost_stable_circular_orbit.
[23] P. I. Jefremov, O. Y. Tsupko, and G. S. Bisnovatyi-Kogan, Innermost stable circular orbits of spinning test particles in Schwarzschild and Kerr space-times, Phys. Rev. D **91**, 124030 (2015).